Supplementary Materials for

S-Scheme Enhanced Photocatalysis On Titanium Oxide Clusters Functionalized with Soluble Perylene Diimides

*Shuqi Dai [a‡], Yongsheng Xu[b ‡], Weijie Zhang[d‡], Shurong Li [e], Qing-yun Guo[f], Jinyi Cui[a], Yaohao Song[a], Jun Yuan[a], Wenchao Peng [b] *, Mingjun Huang [a, c]**

[a] South China Advanced Institute for Soft Matter Science and Technology (AISMST), School of Emergent Soft Matter, South China University of Technology, Guangzhou 510640, China.

[b] School of Chemical Engineering and Technology, Tianjin University, Tianjin 300350, China

[c] Guangdong Provincial Key Laboratory of Functional and Intelligent Hybrid Materials and Devices, South China University of Technology, Guangzhou 510640, China.

[d] Department of Chemistry, University of North Texas, Denton, TX 76203, United States.

[e] Department of Chemistry, College of Chemistry and Chemical Engineering, Xiamen University, Xiamen 361005, China.

[f] Department of Polymer Science, School of Polymer Science and Polymer Engineering, The University of Akron, Akron, OH 44325-3909, USA.

‡ S.-Q. D. and Y.-S. X. and W. J. Z. contributed equally.

*Corresponding author. Email: huangmj25@scut.edu.cn (M. H.); wenchao.peng@tju.edu.cn (W. P.)

Materials and Methods

Materials

All commercial chemicals and solvents were used as received, unless stated otherwise.

Methods

Synthesis of NH_2-TOC: According to previous literatures,[1] the process to obtain NH_2-TOC by following step: A 50 mL vial was charged with $Ti(OBu)_4$ (1.7 mL, 5 mmol), 4-aminobenzoic acid (1.03 g, 7.5 mmol) and 40 ml ethylene glycol to forming clear red solution. The mixtures was put into electric thermostat at 120 ℃ for 48 hr. After cooling down to room temperature, the solvent removed by centrifugal separation. orange red solid was washed by THF for two more times. The orange red powder product was obtained and dried. Yield: 0.98 g (48 %); appearance: orange red powder. FTIR (KBr): v = 3343 (vw), 3216 (vw), 2920 (vw), 2854 (vw), 1602 (w), 1578 (w), 1504 (s), 1387 (s), 1308 (s), 1117 (w), 1073 (m), 1038 (m), 896 (m), 849 (w), 781 (m), 739 (m), 700 (s), 627 (s), 587 (s), 506 (s).

Synthesis of C_{10}-PDI-POSS: According to previous literature,[2] to a 100 mL Schlenk flask charged with perylene-3,4-anhydride-9,10-di-(decyloxycarbonyl) (2.0 g, 2.89 mmol, 1 equiv.), aminopropylisobutyl POSS (3.29 g, 3.76 mmol, 1.3 equiv.) and 20 g imidazole. The mixture was purged with N_2 flow for 15 min. Then 4 mL ODCB was added to the flask and heated to 125 °C with vigorous stir for 12 h. The red mixture was cooled to 90 °C and 60 ml methanol was added. The crude product was separated by filtration and further purified by column chromatography (silica gel) using 20/1 (v/v) $CHCl_3$/Acetone as the eluent. Yield: 4.1 g, 90% (dark red solid). ^1H NMR (400 MHz, $CDCl_3$, ppm, δ): 8.35 (d, 2H, PBI-Ar), 8.10 (t, 4H, PBI-Ar), 7.95 (d, 2H, PBI-Ar), 4.37(t, 4H, $CO_2CH_2CH_2$), 4.21 (t, 2H, $SiCH_2CH_2CH_2$-N), 2.00-1.75 (m, 13H, $SiCH_2CHC_2H_6$ + $SiCH_2CH_2CH_2N$ + $CO_2CH_2CH_2$), 1.52 – 1.25 (m, 28H, $CO_2CH_2CH_2(CH_2)_7CH_3$), 0.96 (d, 42H, $SiCH_2CHC_2H_6$), 0.88 (t, 6H, -CH_3), 0.75 (t, 2H, $SiCH_2CH_2CH_2$-N), 0.65-0.55 (m, 14H, $SiCH_2CHC_2H_6$).

Synthesis of PDI-POSS: According to previous literature,[3] A 50 mL round bottom flask was charged with C_{10}-PDI-POSS (2.0 g, 1.292 mmol), 60 mL toluene and ptoluenesulfonic acid monohydrate (PTSA, 0.54 g, 2.80 mmol). Then the flask was capped and heated to 100 °C under vigorous stir for 12 h. Volatiles were removed on a rotary evaporator, and the solid residue was washed by methanol twice and acetone twice. The solid product after filtration was further purified by column chromatography (silica gel) using 20/1 (v/v) $CHCl_3$/Acetone as the eluent. Yield: 0.82 g, 82% (orange solid). ^1H NMR (400 MHz, $CDCl_3$, ppm, δ): 8.71-8.62 (m, 8H, PBI-Ar-H), 4.21 (t, 2H, $SiCH_2CH_2CH_2$-N), 2.00-1.75 (m, 9H, $SiCH_2CHC_2H_6$ + $SiCH_2CH_2CH_2N$), 0.96 (d, 42H, $SiCH_2CHC_2H_6$), 0.77 (t, 2H, $SiCH_2CH_2CH_2$-N), 0.75-0.60 (m, 14H, $SiCH_2CHC_2H_6$).

Synthesis of NH_2-TOC-PDI-POSS: According to previous literature,[3] A 50 mL Schlenk flask charged with NH_2-TOC (123.8 mg, 0.018 mmol, 1 equiv.), PDI-POSS (404 mg, 0.315 mmol, 17.6 equiv.), DMAP (43.9 mg, 0.36 mmol, 20 equiv.), and12 g imidazole were added. The mixture was purged with N_2 flow for 15 min. Afterward 4 mL ODCB was added and the flask was inserted to oil bath kept at 125 °C for 12 h. The red mixture was cooled to 90 °C and 30 ml

methanol was added. The solid was collected by filtration, washed by methanol twice and acetone twice.

Synthesis of 2D C_3N_4 NanoSheet: According to previous literature,[4] 20 g of urea powder was put into an alumina crucible with a cover and then heated to 550 °C at a rate of 0.5 °C/min in a muffle furnace and maintained at this temperature for 3 h. C_3N_4 was obtained after cooling down to room temperature. The material is dispersed in water for washing, and then suction-filtered to obtain a material. Finally, the sample was lyophilized at -60 °C for 12 h. the 2D C_3N_4 nanosheet was successfully obtained.

Synthesis of TOC-PDI-POSS/g-C_3N_4: Typically, 20 mg TOC-PDI-POSS was dissolved in 2 mL CHCl3 (good solvent) under ultrasonic treatment. Different amount of C_3N_4 (20, 40, 80, 120 mg) was added. Then 20 mL CH_3OH (poor solvent) was poured into the above mixture solution all at once, respectively. Solid insoluble precipitates would appear instantly. After another 0.5 h, and these precipitated dark red solids were collected by filtration through a 0.45 μm membrane filter, washed with CH_3OH for three times, and then lyophilized at -60 °C for 12 h for subsequent use. The as-synthesized products with different adding amount of C_3N_4 were labeled as 1:1, 1:2, 1:4, and 1:6, respectively.

Characterization

Solution Nuclear Magnetic Resonance Spectroscopy (NMR) were carried out by the Varian Mercury 300 MHz. Gel permeation chromatography (GPC) measurements were carried out on a LC98IIRI equipment. The column system was calibrated by a set of monodisperse polystyrene standards. Dynamic light scattering (DLS) measurements were carried out on a Nano Brook Omni instrument. The Inductively coupled plasma mass spectrometry (ICP-MS) measurement of Samples were carried out in Agilent ICPMS 7700. The auxiliary flow and carrier gas are 1.50 L/min and 1.10 L/min, respectively. Before the ICP-MS test, the TOC-PDI-POSS was calcined in air at 800 ^oC for 4h. To determine the hydrodynamic radii of the TOC-PDI-POSS nanoparticles, DLS studies were performed. The samples for this study were prepared by filtering the solutions with a 0.22 μm filter. Possible intermediates were analyzed by liquid chromatography coupled with mass spectrometer (Agilent 1290-6530-Qtof). Total Organic Carbon (TOC) was measured using a TOC-Vmp analyzer (Shimadzu, Japan). All TEM images were obtained on the JEM-F200 with the copper grid (200 mesh). The XRD patterns were obtained on the Bruker D80Focus. The scanning speed is 5^o/min. FTIR spectra were recorded on the Thermo Nicolet 360 and the simples was grinded with KBr (chromatographic grade) for further measurements. UV-vis DRS spectra was recorded on a Shimandzu UV-2550 spectrometer with the range of 200~800 nm. The $BaSO_4$ (chromatographic grade) was used as the background. All XPS spectra were recorded on the Thermo ESCALAB 250Xi with an aluminum X-ray source. In both XPS scpectra of Ti 2p and VB, the powder was pressed into pellets. For UPS spectra, the g-C3N4 was firstly dispersed in water and then coated on the surface of fluorine-doped SnO_2 glass electrode (FTO, 1 cm × 1 cm) for further measurement. ESR was recorded with a Bruker A300. The trapping agent of both radicals is 5,5-dimethyl-1-pyrroline-N-oxide (DMPO, 50 mM). For hydroxyl radicals, the solvent is deionized water while methanol was used for superoxide radicals. The fluorescence spectroscopy (FLS1000, Edinburgh Instruments) was employed to determine the steady and transient state of materials. In both

experiments, the excitation wavelength is 365 nm. Besides, the data of were fitted by three-exponential equation as follows:

$$R(t) = A_1 e^{\left(\frac{-t}{\tau_1}\right)} + A_2 e^{\left(\frac{-t}{\tau_2}\right)} + A_3 e^{\left(\frac{-t}{\tau_3}\right)}$$

Evaluated methods.

Catalytic performance evaluation: In catalytic evaluated system, 25 mg catalyst was added into the 50 mg of phenol solution (5 ppm) with batch stirred reactor. The temperature of whole system was controlled at 298.15 K by circulator bath. The 300 W Xe lamp was purchased in CEAULight with AM 1.5G light filter and the distance between light filter and the reactant surface is 20 cm. The solution was stirred for one hour under dark condition, then 0.5 mL reactant irradiation was injected into 0.5 mL methanol at every intervals. The mixture was filtered by 0.22 μm organic membrane and the filtrate was analyzed by high performance liquid chromatography (HPLC, Thermo U3000). The condition of HPLC is as follows: mobile phase is acetonitrile/water (4:6) with the flow velocity of 1 mL/min and the detected wavelength is 220 nm. Besides, the catalyst was collected after every cycle without any other washing. The quenching agents are both 5 mM and added into solution before reaction.

Photoelectrochemical evaluation: The photoelectrochemical experiments (photocurrent and EIS experiments) were measured on a three-electrode system with an CHI660E electrochemical workstation (Shanghai Chenhua). An Ag/AgCl electrode, carbon electrode, and FTO electrode (1 cm × 2 cm, the coating area of catalyst was 1 cm^2) were used as the reference electrode, counter electrode and working electrode, respectively. 50 mL of 5 ppm phenol solution was used as electrolyte. In the photocurrent experiments, the light source was the same as catalytic evaluation process and the time of light cycle was 30 s. In EIS experiments, the frequency range was between 0.1~1000000 Hz.

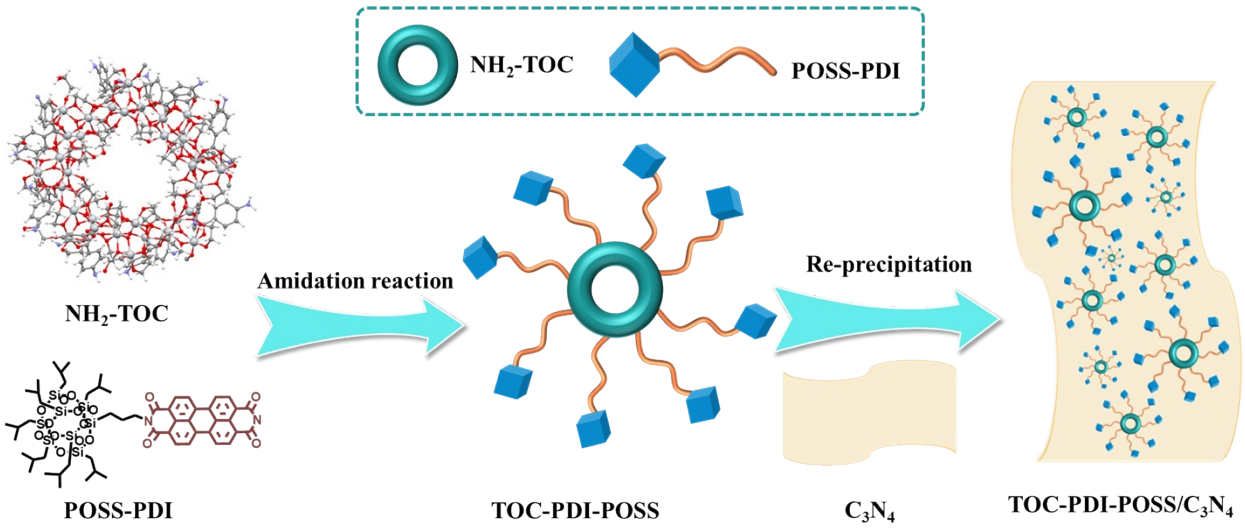

Scheme S1. Schematic illustration for the synthesis of TOC-PDI-POSS/g-C_3N_4 heterostructure.

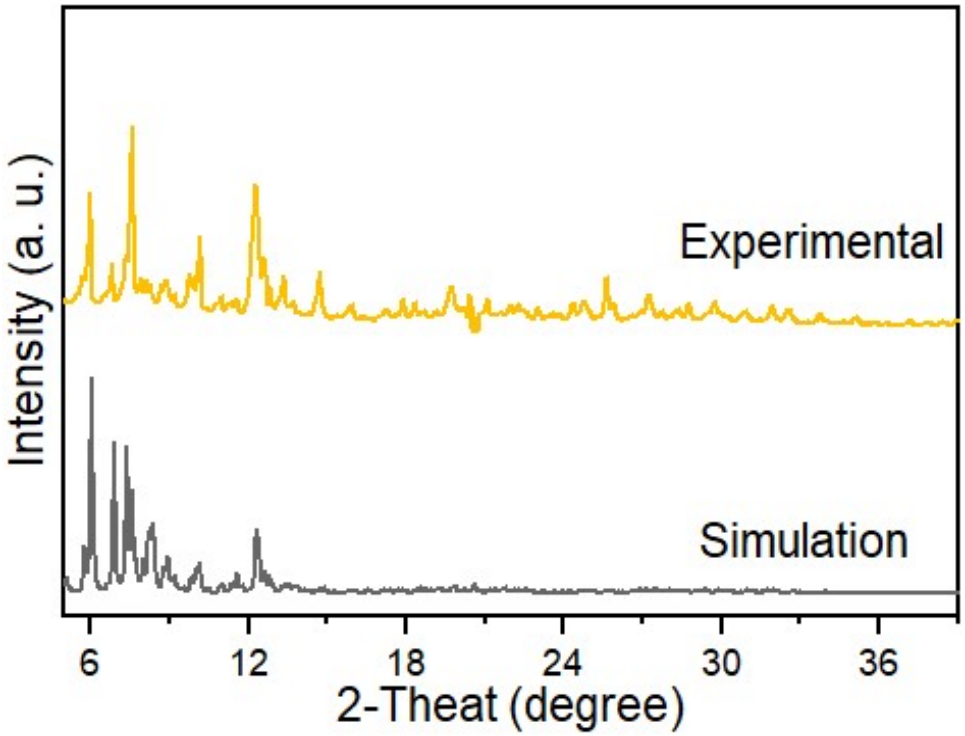

Figure S1. Experimental and simulated powder X-ray diffraction of NH_2-TOC.

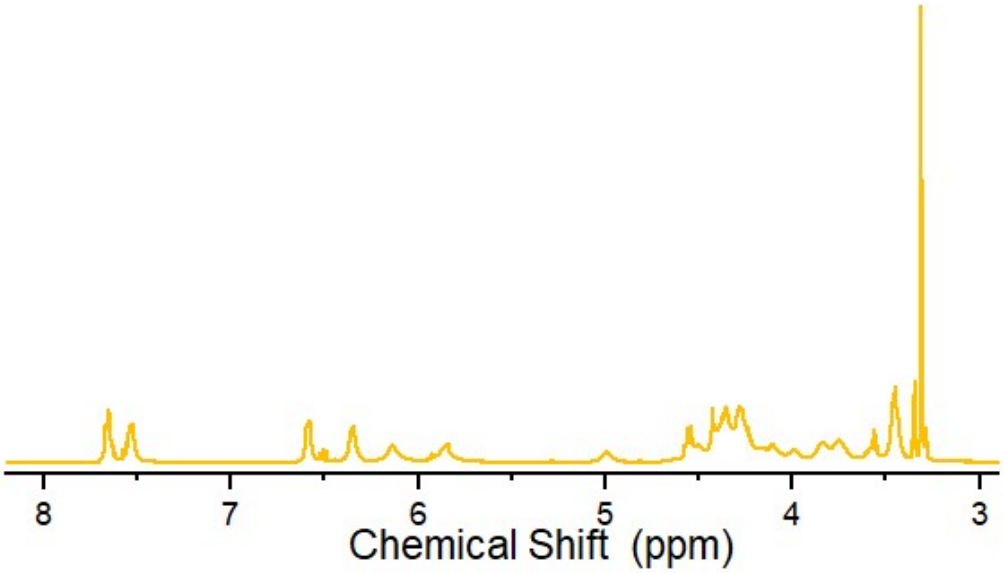

Figure S2. ^{1}H NMR of NH_2-TOC in DMSO-d6 after solvent washed with THF followed by vacuum drying.

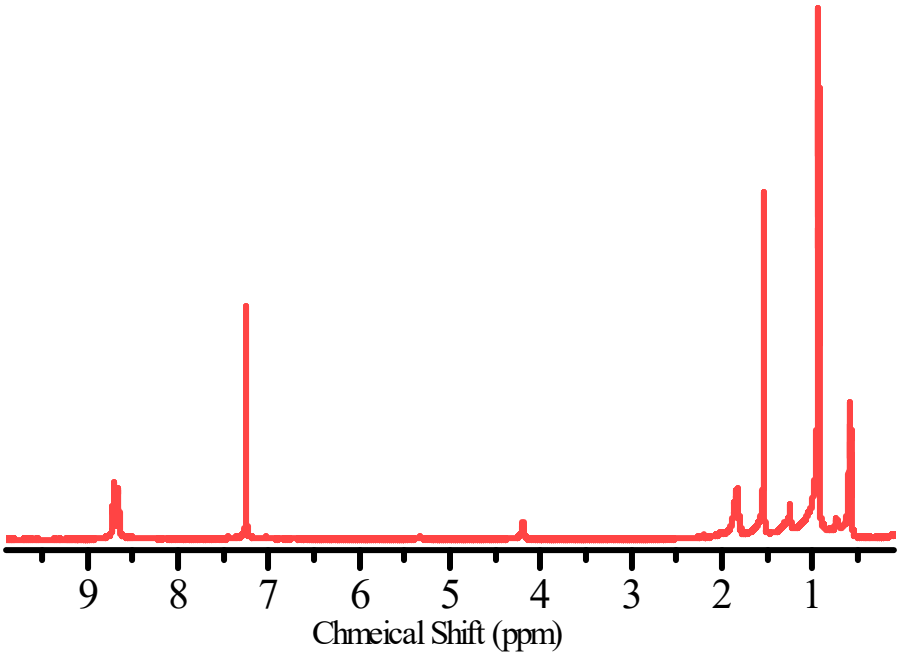

Figure S3. ^{1}H NMR of TOC-PDI-POSS in $CDCl_3$ solution.

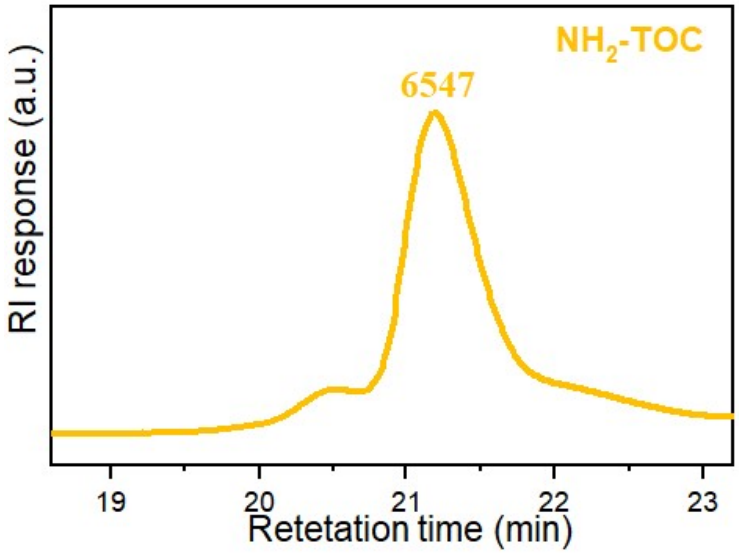

Figure S4. GPC of NH_2-TOC in DMF solution.

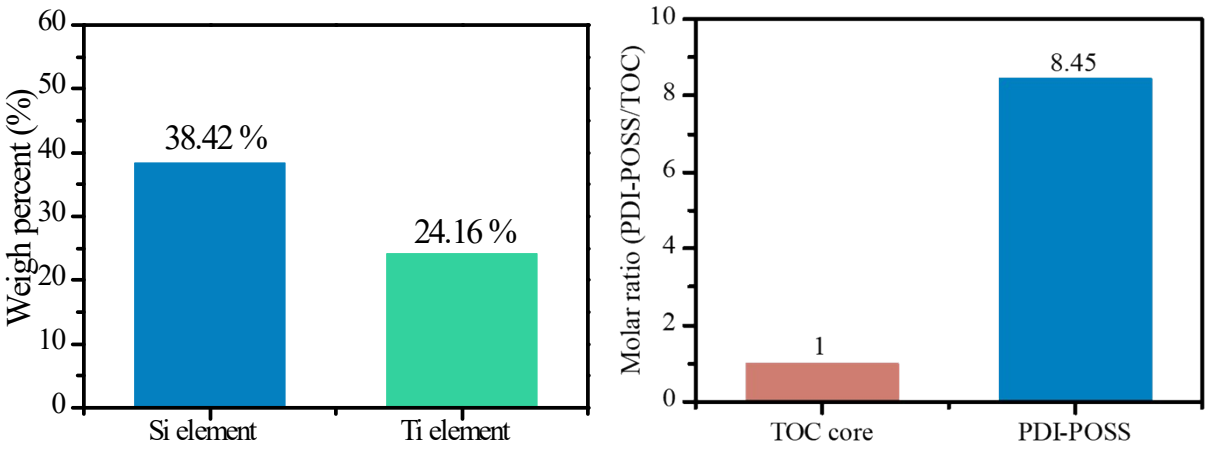

Figure S5. The weight percent of silicon (Si) and Titianium (Ti) in TOC-PDI calcined at 800 °C (left). The molar ratio of PDI-POSS and TOC.

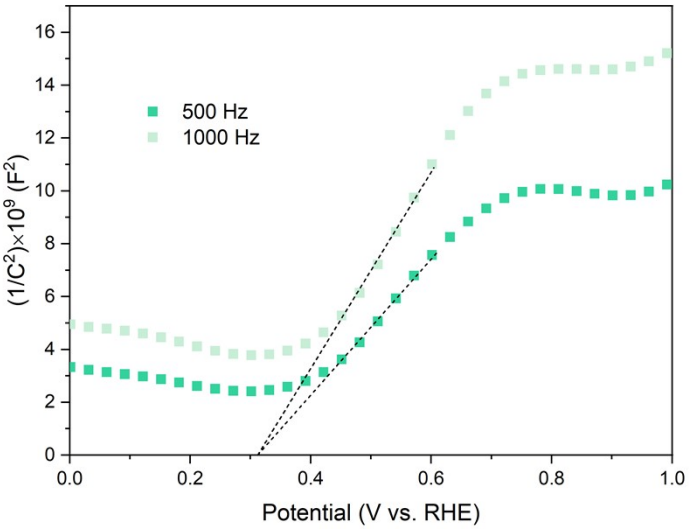

Figure S6. Mott-Schottky plot of TOC-PDI-POSS.

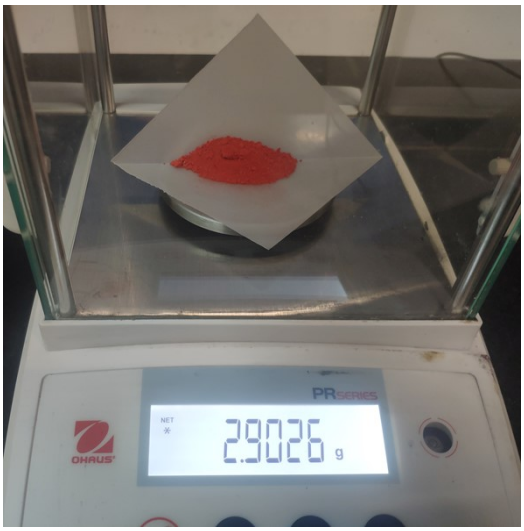

Figure S7. One-pot synthesis of grame-scale TOC-PDI-POSS/C_3N_4 heterostructure (1:2).

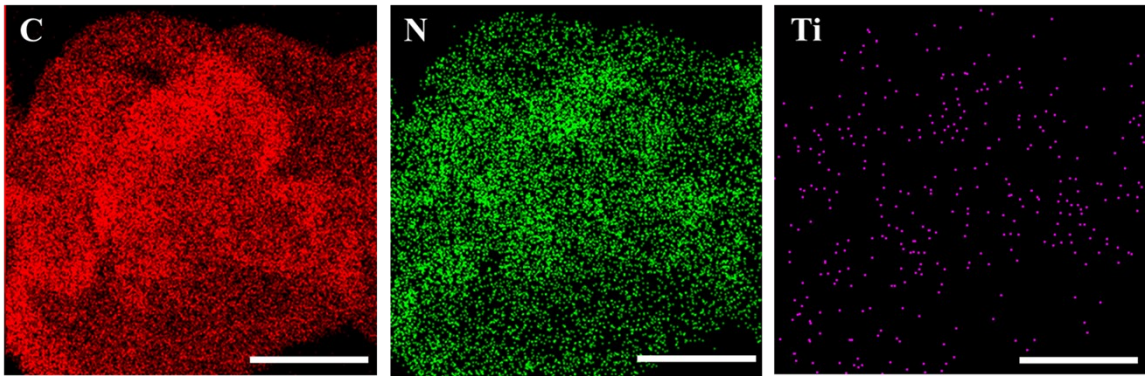

Figure S8 EDS elements mappings of TOC-PDI-POSS/g-C_3N_4 heterostructure (1:2) and (Scale: 100 nm).

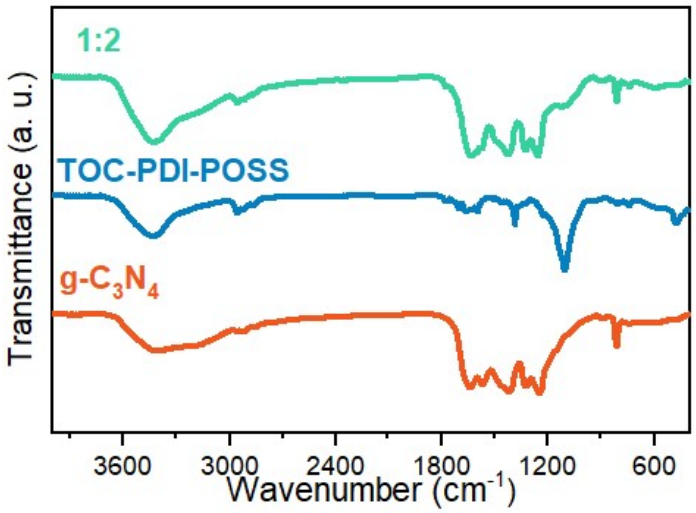

Figure S9. FT-IR spectrum of NH_2-TOC-PDI-POSS NH_2-TOC and TOC-PDI-POSS/g-C_3N_4 heterostructure (1:2).

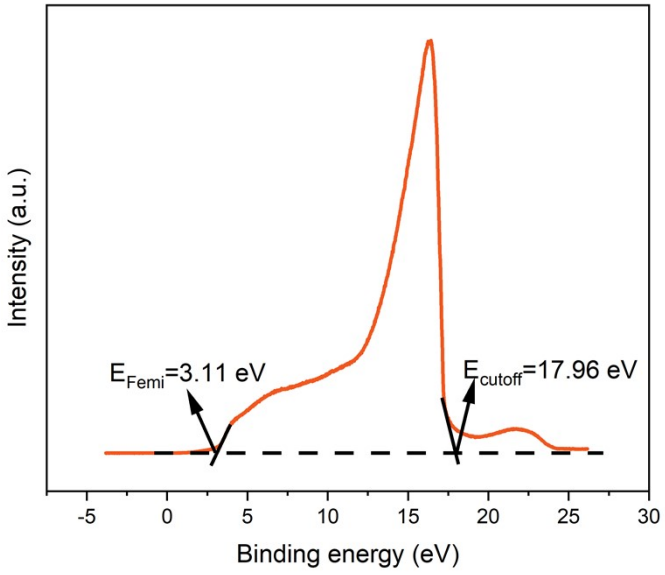

Fiugre S10. UPS spectrum of g-C_3N_4.

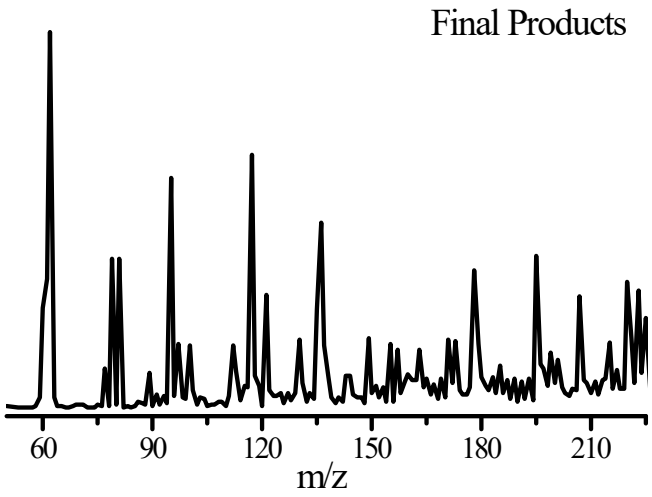

Figure 11. LC-MS spectra of final products for photocatalytic phenol degradation.

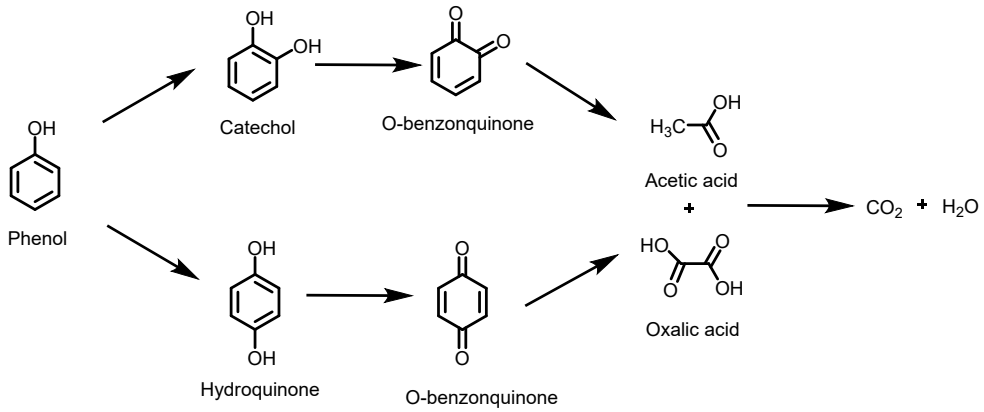

Figure S12. Proposed photocatalytic degradation pathways of phenol.

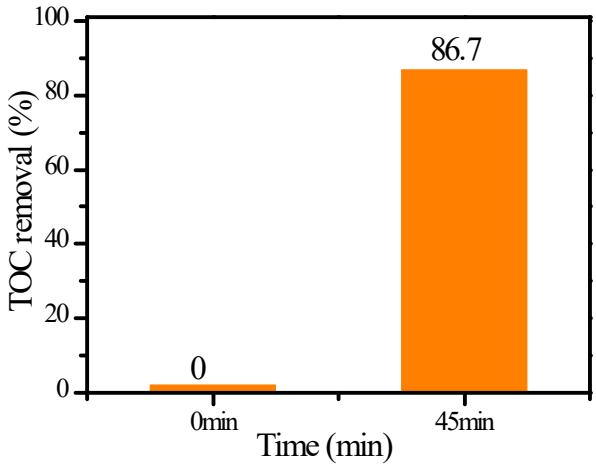

Figure S13. TOC removal with heterostructure (1:2) as activator in 0 and 45 min. (The reaction conditions: [phenol] = 20 ppm, [activator] = 0.5 mg/L, T = 25 ºC.)

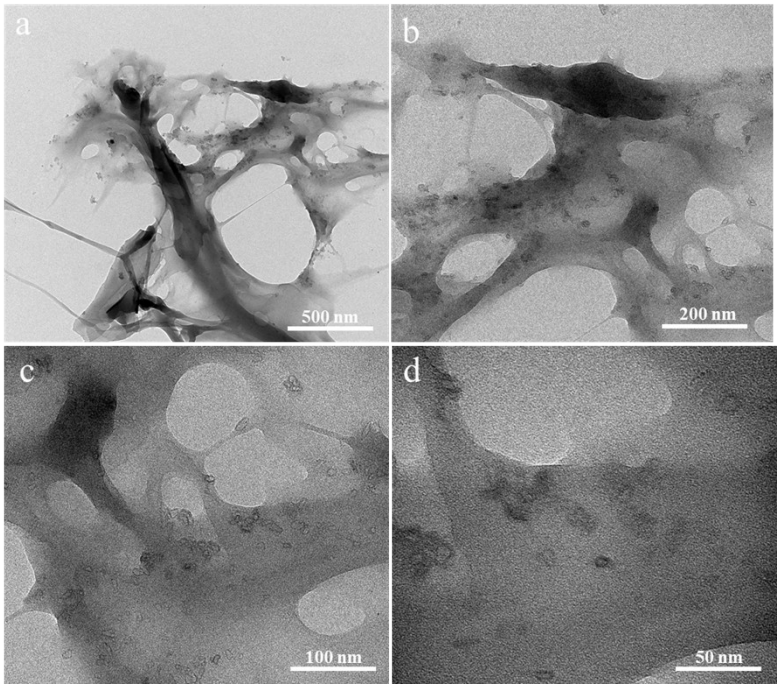

Figure S14. TEM images of TOC-PDI-POSS/C_3N_4 after the photocatalysis with different scales.

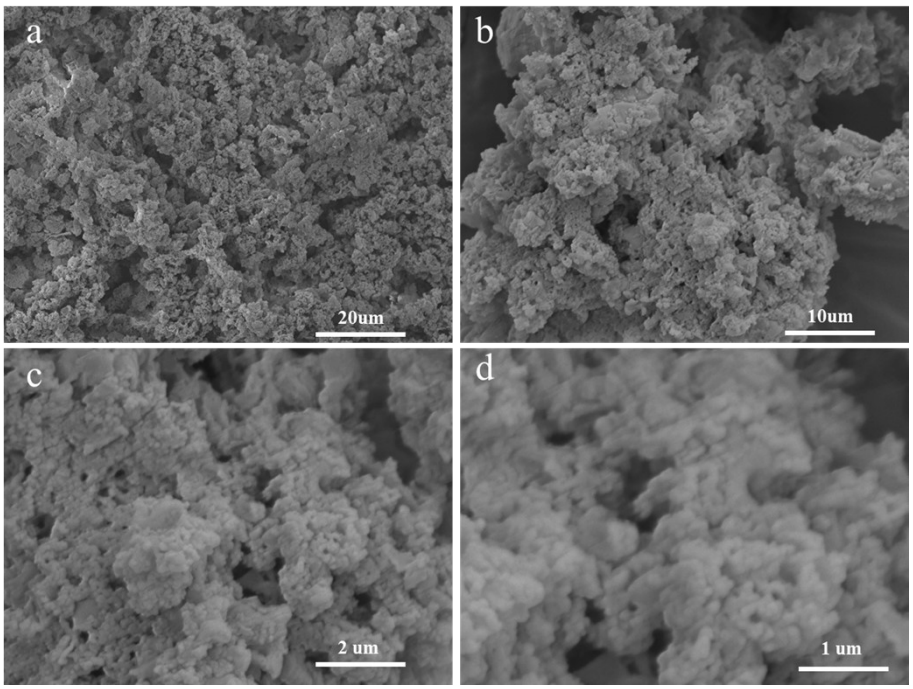

Figure S15. SEM images of TOC-PDI-POSS/C_3N_4 after the photocatalysis with different scales.

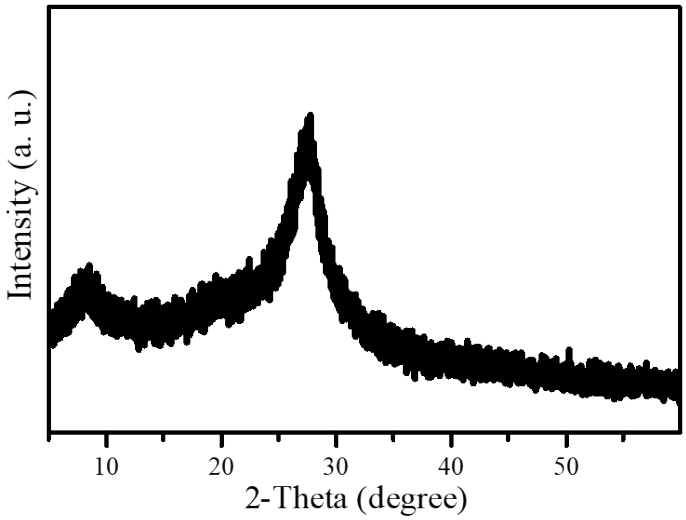

Figure S16. the XRD spectrum of TOC-PDI-POSS/C_3N_4 after the photocatalysis.

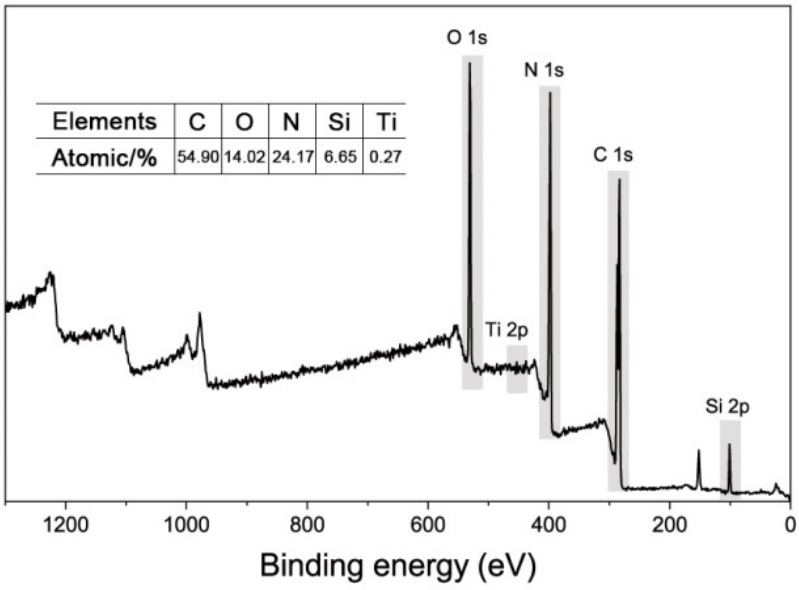

Figure S17. XPS survey spectrum of used TOC-PDI-POSS/C_3N_4.

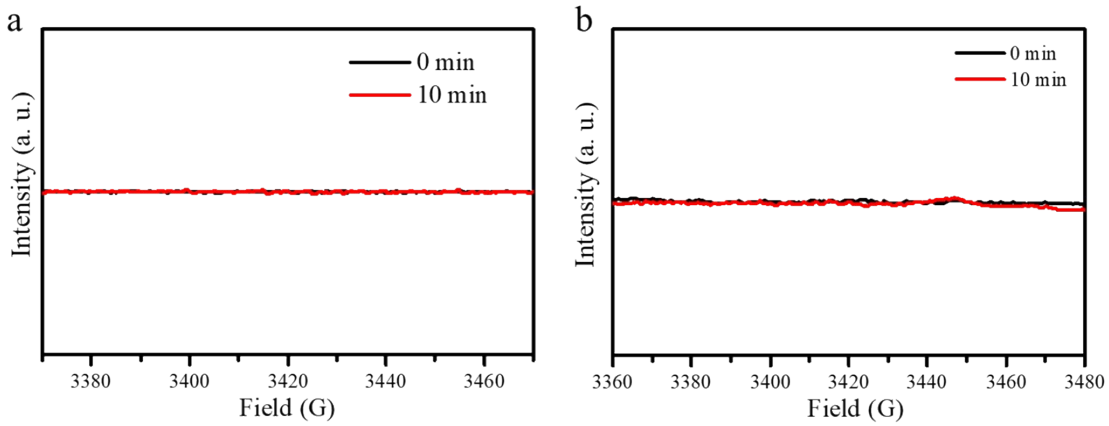

Figure S18. ESR spectra of $O_2^{\bullet-}$ in the and (b) $^{\bullet}OH$ in the PDI-TOC-POSS.

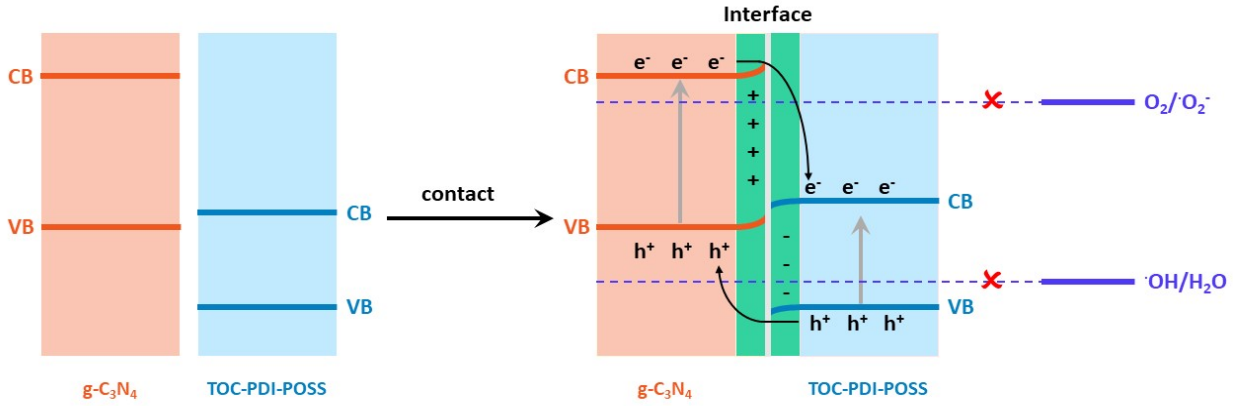

Figure S19. Schematic of the type II charge-transfer route in the PDI-TOC-POSS/g-C_3N_4 heterostructure.

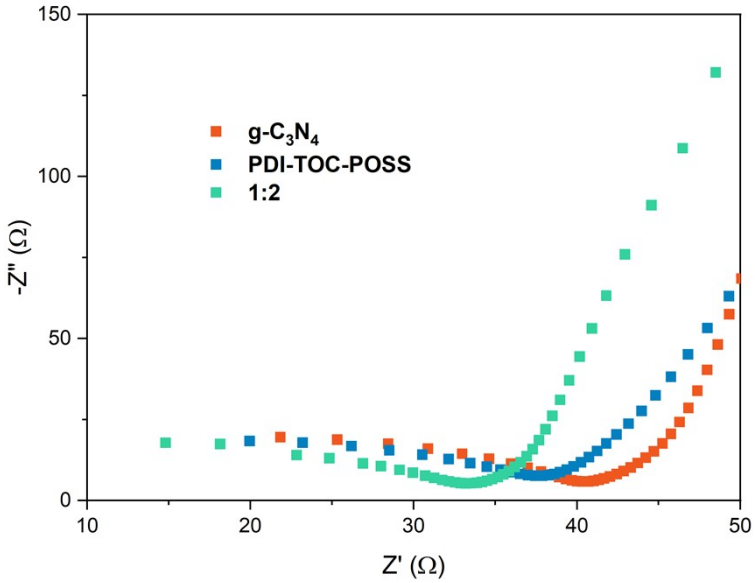

Fiugre S20. Electrochemical impedance spectroscopy (EIS) Nyquist plots of catalysts.

Table S1. Performance comparison between TOC-PDI-POSS heterojunction and other heterojunction designs.[5-13]

Catalyst		Heterojunction Type	Reaction rate (mL mg^{-1} h^{-1})	Organic pollutant	Light	Reference
Composition I	Composition II					
PDI	oxygen-doped g-C_3N_4	Type II	0.328	Phenol (5 ppm)	500 W xenon lamp ($\lambda > 420$ nm)	5
WO_3	g-C_3N_4	Z-scheme	3.6	Methylparaben (10 ppm)	500 W xenon lamp ($\lambda > 400$ nm)	6
π-conjugated PDI	/	/	2.46	Phenol (5 ppm)	300 W xenon lamp ($\lambda > 420$ nm)	7
PDI	Bi_2WO_6	Type II	0.72	Phenol (5 ppm)	500 W Xe lamp ($\lambda \geq 420$ nm)	8
PDI	BiOCl	Type II	0.44	Phenol (5 ppm)	800 W Xe lamp ($\lambda \geq 420$ nm)	9
PDI	BiOCl	S-scheme	0.78	Phenol (5 ppm)	300 W Xe lamp ($\lambda \geq 420$ nm)	10
PDI	TiO_2	Type II	0.2	Phenol (5 ppm)	300 W Hg lamp (190-1100 nm)	11
PDI	Reduced graphene oxide	/	0.96	Phenol (5 ppm)	500 W Xe lamp ($\lambda \geq 420$ nm)	12
PDI	graphene quantum dots		2.16	Phenol (5 ppm)	500 W Xe lamp ($\lambda \geq 420$ nm)	13
TOC-PDI-POSS	g-C_3N_4	S-scheme	10.12	Phenol (5 ppm)	300 W xenon lamp (AM 1.5G)	**This work**

Table S2. Parameters of average fluorescence lifetime for g-C_3N_4 and heterostructure (1:2).

	A_1	τ_1 (ns)	A_2	τ_2 (ns)	A_3	τ_3 (ns)	τ_{avg} (ns)
g-C_3N_4	4382.74	1598.21	85.10	0.51	2.47	13.09	3.48
heterostructure (1:2)	3012.45	1603.77	179.40	1.12	5.06	20.61	7.97

Equation of hydroxyl radical formation:

$$OH^- + h^+ \longrightarrow {}^{\bullet}OH$$

Equation of superoxide radical formation:

$$O_2 + e^- \longrightarrow O_2^{\bullet -}$$

Text S1. Formation of hydroxyl and superoxide radicals.

References

[1] J. Li, S. Dai, R. Qin, C. Shi, J. Ming, X. Zeng, X. Wen, R. Zhuang, X. Chen, Z. Guo, X. Zhang, *ACS Appl Mater & Interace* 2021 **13** 54727-54738.

[2] C. Xue, R. Sun, R. Annab, D. Abadi, S. Jin, *Tetrahedron Lett* 2009 **50** 853-856.

[3] J. Huang, H. Ren, R. Zhang, L. Wu, Y. Zhai, Q. Meng, J. Wang, Z. Su, R. Zhang, S. Dai, S. Z. D. Cheng, M. Huang, *ACS Nano* 2020 **14** 8266-8275.

[4] L. Wang, X. Zhang, X. Yu, F. Gao, Z. Shen, X. Zhang, S. Ge, J. Liu, Z. Gu, C. Chen, *Adv Mater* 2019 **31** 1901965.

[5] Q. Gao, J. Xu, Z. Wang, Y. Zhu, *Appl. Catal. B Environ* 2020 **271** 118933.

[6] J. Meng, X. Wang, Y. Liu, M. Ren, X. Zhang, X. Ding, Y. Guo, Y. Yang, *Chem. Eng. J.* 2021 **403** 126354.

[7] Y. Zhang, D. Wang, W. Liu, Y. Lou, Y. Zhang, Y. Dong, J. Xu, C. Pan, Y. Zhu, *Appl. Catal. B Environ* 2022 **300** 120762.

[8] K. Zhang, J. Wang, W. Jiang, W. Yao, H. Yang, Y. Zhu, *Appl. Catal. B Environ* 2018 **232** 175-181.

[9] Q. Ji, Z. Xu, W. Xiang, Y. Wu, X. Cheng, C. Xu, C. Qi, H. He, J. Hu, S. Yang, S. Li, L. Zhang, *Chemosphere* 2020 **253** 126751.

[10] X. Gao, K. Gao, X. Li, Y. Shang, F. Fu, Catal Sci. Technol 2020 **10** 372-381.

[11] W. Wei, Y. Zhu, *Small* 2019 **15** 1903933.

[12] J. Yang, H. Miao, Y. Wei, W. Li, Y. Zhu, *Appl. Catal. B Environ* 2019 **240** 225-233.

[13] J. Yang, H. Miao, J. Jing, Y. Zhu, W. Choi, *Appl. Catal. B Environ* 2021 **281** 119547.